



Removal of Lead(II) by Phyto-inspired Iron Oxide Nanoparticles

Merina Paul Das[†] and L. Jeyanthi Rebecca

Department of Industrial Biotechnology, Bharath University, 173 Agaram Road, Selaiyur, Chennai-600 073, T. N., India

[†]Corresponding author: Merina Paul Das

Nat. Env. & Poll. Tech.

Website: www.nepjtjournal.com

Received: 01-08-2017

Accepted: 25-09-2017

Key Words:

Trigonella foenum-graecum

Iron oxide nanoparticles

Lead

Adsorption

ABSTRACT

Heavy metals are toxic to the living bodies even though present in trace amounts. In this study, we have developed a simple approach for the biosynthesis of iron oxide nanoparticles (Fe_3O_4 -NPs) using *Trigonella foenum-graecum* leaf extract and used it for possible removal of lead from aqueous solution and wastewater. SPR peak at 248 nm confirms the bioreduction and formation of Fe_3O_4 -NPs. The shape and size of the nanoparticles were evaluated by SEM equipped with EDX, TEM, XRD. The particles were found crystalline and roughly spherical in shape with an average size range of 51.6-215.7 nm. The possible biomolecules participated in the biosynthetic reaction which was confirmed by FTIR spectrum. These nanostructured particles were used for batch adsorption study for the removal of lead ions. The effects of various physical and chemical parameters like pH, contact time, adsorbent dosage and initial concentrations on the removal of heavy metals were studied on removal efficiency. The maximum lead(II) ions removal uptake was found $93 \pm 0.13\%$ at pH 6.0 with 0.4g of these nanoparticles within 60 min of contact time. Desorption studies indicated that the regenerated nanoparticles retained its original metal adsorption efficiency. Results showed that these regenerable iron oxide nanoparticles can be used as nano-adsorbent for removal of heavy metals from environmental waste due to its high metal uptake capacity.

INTRODUCTION

Metal and metal oxide nanoparticles have been attracting a great deal of attention due to their noble properties and unique potential applications in the fields of biological labelling, environmental pollution control, photography, catalysis, photonics, drug delivery carrier, optoelectronics, etc. (Gittins et al. 2000). Among them, iron oxide nanoparticles (Fe_3O_4 -NPs) have received significant importance because of their multitasking properties such as superparamagnetic, biodegradable, and biocompatibility (Mahdavian & Mirrahimi 2010, Chang et al. 2011), and are used as catalyst, biosensor, magnetic resonance imaging agent, drug carrier, etc. (Gawande & Varma 2013, Weiss & Ranke 2002, Vicky et al. 2010). The sensitivity of the nanomaterials in various applications can be enhanced by controlling shape and morphology, chemical composition, and dispersities (Ahmed et al. 2003). Thus, the control over the synthetic reaction is very much important to achieve the tunable structure of nanoparticles. Conventionally, Fe_3O_4 -NPs have been synthesized and stabilized by a different number of physical and chemical methods, such as solid state synthesis (Paiva et al. 2015), hydrothermal process (Hua & He 2008) and electro-chemical route (Franger et al. 2004). Indeed, phyto-inspired synthesis methods are most accepted one because of their simplicity, non-toxicity and cost-effective nature.

Rapid industrialization leads to a huge amount of generation and disposing of wastes, especially heavy metal wastes causing environmental pollution and a serious threatening to human health (Jose et al. 2017). Lead (Pb) is considered as one of the major industrial pollutants that penetrate into ecosystems through air, soil and water. According to World Health Organization (WHO), the permissible level of Pb(II) is 0.1 mgL^{-1} in drinking water sources (WHO 1984). Pb(II) toxicity in living organisms causes changes in proteins and nucleic acid conformation, cellular enzyme inhibition, dysfunction of cell membrane, change in osmotic balance and interferes with cellular metabolism (Bruins et al. 2000). Several traditional adsorption methods are used to remove the heavy metals, but these processes have some disadvantages like cost-intensive, high energy requirements, generation of toxic by-products, and incomplete metal removal (Bai & Abraham 2003). Thus, in recent years, much interest has been exhibited in the use of nano sized metal oxides for removal of heavy metals from aqueous systems (Hua et al. 2012).

MATERIALS AND METHODS

Chemicals: Iron chloride hexahydrate ($\text{FeCl}_3 \cdot 6\text{H}_2\text{O}$) and lead nitrate ($\text{Pb}(\text{NO}_3)_2$) were procured from Sigma-Aldrich (India). All these chemicals with analytical grade were directly used in experiments without any purification. Glassware were washed with distilled water, followed by chromic

acid and dried in oven prior to use. Young leaves of *Trigonella foenum-graecum* have been collected from local crop field of Chennai, India. Wastewater was collected from the industrial zone near Nagalkeni (Longitude 80°8'13" E; Latitude 12°57'39" N), Chennai.

Green synthesis of iron oxide nanoparticles: Fresh *T. foenum-graecum* leaves were thoroughly washed, dried and ground for preparation of leaf extract. Five g of leaf powder was mixed with 100 mL of distilled water in 250 mL of conical flask and heated at 60°C for 15 min. Then the obtained solution was centrifuged at 4000 rpm for 15 min and used for metal oxide nanoparticle synthesis. 0.1 M aqueous solution of FeCl₃ was added dropwise to the *Trigonella* leaf extract (TLE) in 1:5 ratio with constant vigorous stirring at 37°C for 30 min. The change in colour from colourless FeCl₃ to black colour indicates the synthesis of Fe₃O₄-NPs. These nanoparticles were separated from resulting colloidal metal oxide suspension, washed with water, ethanol and finally dried under vacuum.

Chemical analysis of Fe₃O₄-NPs: Spectral analysis of biosynthesized metal nanoparticles was recorded within a range 300-700 nm using double beam UV-visible spectrophotometer; the size and morphology of Fe₃O₄-NPs were observed by scanning electron microscopy (SEM) and transmission electron microscopy (TEM); the elemental composition and crystallinity of the metal oxide nanoparticles were analysed by energy dispersive X-ray (EDX) and X-ray diffraction (XRD) spectrum. The functional groups in the biomolecules present in the TLE involved in the Fe₃O₄-NPs biosynthesis were verified by Fourier transform infrared spectroscopy (FTIR).

Batch adsorption studies: The stock solution of 1 g/L of lead (II) ions was prepared using pure Pb(NO₃)₂ with distilled water. The batch study for removal of lead was carried out by exposing to the lead ions with constant agitation at 150 rpm at 27°C. The influence of various parameters like pH, exposure time, initial metal concentration, and adsorbent dose on metal adsorption by Fe₃O₄-NPs was checked. Adsorption experiments were performed at different pH levels (3, 4, 5, 6, 7, 8) by adjusting with 1N HCl and NaOH, contact time (30, 60, 90, 120, 150, 180 min), initial lead (II) concentration (25, 50, 100, 150, 200, 250 mg/L) and adsorbent dose (0.1, 0.2, 0.3, 0.4, 0.5 g/100 mL). At the end of the reaction, the iron oxide metal nanoparticles were separated from the solution using magnet, and residual amount of Pb(II) was determined by atomic adsorption spectrophotometer (AAS) at 217 nm. The heavy metal removal efficiency of Fe₃O₄-NPs was calculated before and after the adsorption using following formula:

$$\text{Removal efficiency (\%)} = \frac{C_i - C_e}{C_i} \times 100$$

Where, C_i and C_e is initial and remaining heavy metal concentrations (mg/L) in solution, respectively.

Removal of Pb(II) from industrial wastewater: Batch adsorption experiment was carried out using optimum conditions such as pH, exposure time, adsorbent dose that affect the adsorption, as obtained from previous test. 100 mL of industrial wastewater containing Pb(II) was incubated with optimum amount of Fe₃O₄-NPs for respective time in an orbital shaker. The initial and final Pb(II) ion concentration of treated wastewater was determined.

Desorption of heavy metal loaded Fe₃O₄-NPs: Desorption of heavy metals from adsorbed iron oxide nanoparticles was carried out for each metal adsorbed sample. The known amount of Pb(II) adsorbed in nanoparticles was separated by filtration, washed with distilled water and finally mixed with 0.1 M HCl and agitated in shaker incubator at room temperature, until desorption was obtained (Silva et al. 2008). Heavy metal concentration was assayed by AAS. At the end of the process, the Fe₃O₄-NPs were regained and checked for adsorption capacity. The desorption efficiency was determined using following equation:

$$\text{Desorption efficiency (\%)} = \frac{\text{Amount of Pb (II) ions desorbed}}{\text{Amount of Pb (II) ions sorbed}} \times 100$$

RESULTS AND DISCUSSION

UV-vis spectroscopic analysis: Green synthesis reaction is the most simple and safest approach to synthesize iron oxide nanoparticle. As the plant biomolecules are involved in synthesis and stabilization of nanoparticles, in the present study, Fe₃O₄-NPs were biosynthesized using aqueous leaf extract of *T. foenum-graecum* with precursor molecule FeCl₃. Formation and stabilization of aqueous solution of metal/metal oxide nanoparticles can be confirmed by UV-vis spectra. The appearance of black colour indicates the bioreduction reaction and biosynthesized iron oxide particles were separated by piece of magnet (Fig. 1a). The characteristic strong surface plasmon resonance (SPR) peak at 248 nm confirms the synthesis of nano iron oxide particles (Fig. 1b). The maximum absorption (λ_{max}) spectrum appeared within a short span of time (30 min), indicates the rapid biosynthesis process.

Characterization of Fe₃O₄-NPs by electron micrograph: The advancement of nanomaterials depends on its size and shapes. Thus, determination of size and morphology of nanoparticles using electronic microscopy is very essential to apply them in various emerging fields. The FE-SEM micrograph shows the distinct morphology of Fe₃O₄-NPs

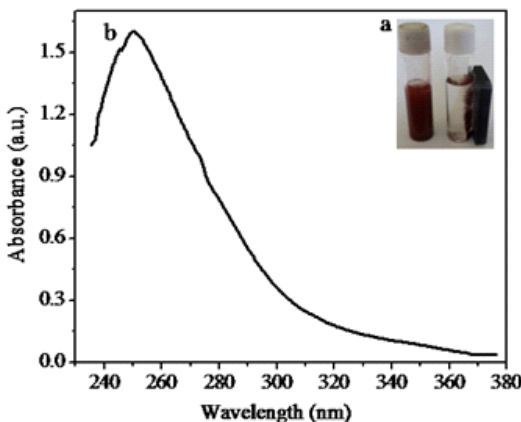


Fig. 1: (a) Color changes after the bioreduction process, and (b) UV-vis spectrum of Fe_3O_4 -NPs synthesized by treating FeCl_3 solution with *T. foenum-graecum* leaf extract.

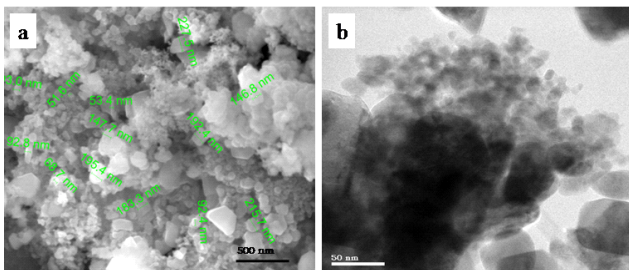


Fig. 2: (a) FE-SEM and (b) TEM micrograph of phyto-inspired Fe_3O_4 -NPs.

(Fig. 2a). It also reveals that metal oxide particles were grown in high density with little aggregation. To get more clear detail about shape, structure of the nanoparticles, the sample was analysed using TEM. TEM images exhibit that almost all particles possess roughly spherical shape (Fig. 2b). The diameter of the Fe_3O_4 nanoparticles was found in the range 51.6-215.7 nm.

Energy dispersive X-ray spectrum of Fe_3O_4 -NPs: Fig. 3 depicts the EDX spectrum of iron oxide nanoparticles. The presence of intense signal at 0.8, 6.2 and 6.9 keV confirms the elemental Fe and at 0.6 confirms the elemental O in Fe_3O_4 nanoparticles. This EDX result also supports the bioreduction reaction. The additional peaks for Cl may be from FeCl_3 and C may be from phytoconstituents, were observed. The elemental percentage from EDX quantification was found 10.34 % of Fe, 49.87 % of O, 6.12 % of Cl, and 33.67 % of C.

X-ray diffraction studies: XRD provides the information about crystal nature of metal oxide nanoparticles and determine the average crystal particle size. Fig. 4 shows the XRD spectrum of Fe_3O_4 -NPs synthesized using TLE. The parti-

cles showed characteristic 2θ peaks at 32.12°, 34.67°, 44.5°, 53.12°, 56.5°, 62.9°, corresponding to the crystalline planes (200), (311), (400), (422), (511), (440), respectively, found to be supported by JCPDF file No. 04-0755 (Zhang et al. 2009) for cubical geometry of Fe_3O_4 -NPs. The intensity of well-defined peaks indicates the crystallinity of the iron oxide nanoparticles and the broadened diffraction peaks confirms the tiny size of the nanoparticles (Wani et al. 2011).

FTIR spectroscopy analysis: FTIR spectroscopy analysis was carried out to identify the possible biomolecules responsible for the reduction of iron ions and capping agent which stabilize the iron oxide nanoparticles synthesized by using *T. foenum-graecum* leaf extract. The absorption peaks of synthesized Fe_3O_4 -NPs are located at 3402, 1628, 1412 and 1065 cm^{-1} in the FTIR spectrum. Fig. 5 suggests that there is presence of -OH stretching vibration (Prathna et al. 2011), flavanones (Rajakumar et al. 2011) which might be responsible for the reduction reaction, methylene scissoring vibration from the proteins in the solution and primary amine C-N stretching vibration (Fayaz et al. 2010) of the proteins, respectively.

Biosorption test: In this report, the biosynthesized Fe_3O_4 -NPs were used to remove Pb(II) ions in aqueous solution by a batch system. To get maximum removal efficiency, various essential physico-chemical parameters like pH, contact time, adsorbent dose and initial metal concentration were tested.

The influence of solution pH on sorption of Pb(II) ions: pH is considered as one of the effective factors that influences biosorption of heavy metals in aqueous solution. The hydrogen ion concentration affects solubilization and ionization of heavy metal ions in solution, and present ionization state on adsorbent surface which determines the availability of metal active site (Repo et al. 2010). In order to assess the effect of pH on removal of lead ions using Fe_3O_4 -NPs, the test was carried out within the pH range 3-8. For each test, other operational factors like amount of iron oxide nanoparticles was kept 0.5 g/100 mL, 90 min of contact time and 25 mg/L of initial lead concentration. After the biosorption, the heavy metal removal efficiency was determined and depicted in Fig. 6. The results revealed that at low pH, the high acidic environment in solution reduces the efficiency of Fe_3O_4 -NPs to adsorb the heavy metals. This may be due to the electrostatic repulsion between positively charged hydrogen ions and Pb^{2+} ions. In presence of high H^+ concentration, Pb(II) ions are replaced by proton on the adsorbent site, thus reducing removal efficiency. But as the pH values were increased from 3 to 6, the adsorption capacity of nanoparticles was increased. The optimum pH was found at 6 where the lead(II) ions were removed about 89.67

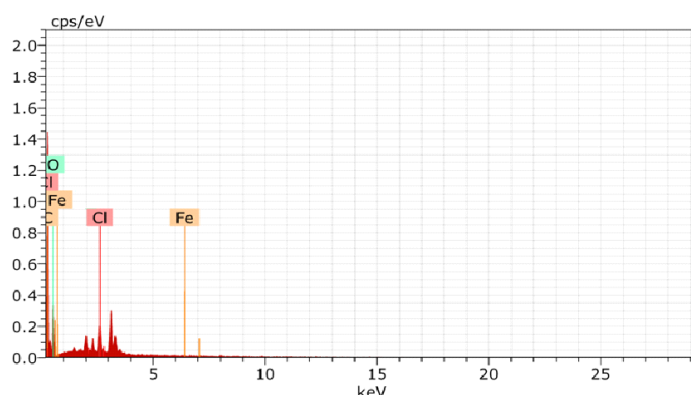


Fig. 3: EDX profile of iron oxide nanoparticles.

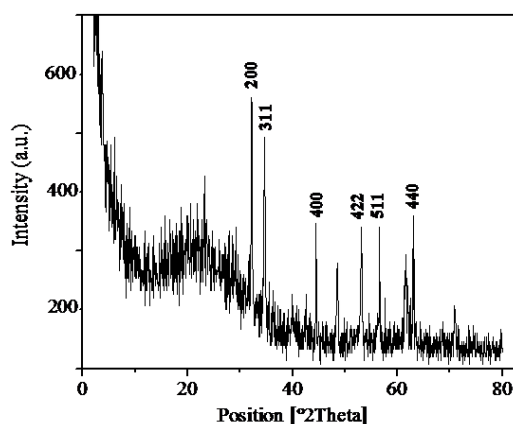


Fig. 4: XRD pattern of biosynthesized iron oxide nanoparticles.

$\pm 0.4\%$. At this pH, due to low hydrogen ion, the functional groups on adsorbent binding site were available to bind with heavy metal and can form metal-chelate complex (Selatnia et al. 2004). This optimal pH value was used for the further studies. At the pH values higher than the optimum pH, there is again reduction in heavy metal removal due to attraction of metal ions to be deposited as Pb(OH)_2 before adsorbing on the Fe_3O_4 -NPs.

Effect of contact time for lead ions removal: Fig. 7 shows the removal efficiency of Pb(II) from aqueous solution using nano iron oxide particles at different contact times of 30, 60, 90, 120, 150, 180 min. For respective period of time study, other adsorption factors such as initial metal ion concentration (25 mg/L) and adsorbent biomass (0.5 g/100 mL) were set with optimum pH 6.0. According to the result, rate of removal efficiency increases with time and the optimal contact time reaches the equilibrium occurred in 60 min. The presence of large number of active binding sites on the biosynthesized Fe_3O_4 -NPs surface makes it prone to attach with heavy metal ions. Finally, the uptake of metal by the nanoparticles becomes constant. This is because of the steric

hindrance between adsorbed metal ions on adsorbent active site and remaining toxic Pb(II) ions in solution. The binding sites were simultaneously exhausted by toxic metal ions, leads to lesser removal efficiency. The maximum exposure time was used in further tests. The similar result was also found by Zhang et al. (2011).

Effect of adsorbent amount on sorption of Pb(II) ions: The influence of adsorbent dose on removal of lead ions was investigated using Fe_3O_4 -NPs as adsorbent within the range from 0.1 g to 0.5 g and initial metal concentration 25 mg/L at pH 6.0 for 60 min. Fig. 8 depicts the increase in percentage of removal efficiency of adsorbate with increase in adsorbent dosage, the significant adsorption was observed up to 0.4 g of metal oxide nanoparticles mass and after that, the adsorption became non-significant. The results indicate the large number of metal binding sites on the adsorbent enhancing the heavy metal adsorption efficiency. Nanoparticles have higher surface area/volume ratio which make them ideal adsorbent to adsorb maximum amount of adsorbate than any other sorbent. But at 0.5 g of nanoparticles, the adsorption capacity rate not so high, this attributed to that some adsorption sites remained unsaturated during the adsorption process. This may be due to the reducing efficiency of adsorbed metal per unit mass of adsorbent (Bulut & Aydin 2005); this phenomena is very common for a batch system. The results imply that even increase in adsorbent amount after obtaining the maximum heavy metal adsorption, the amount of adsorbed ions and remaining unbound ions become constant, even after further increment of adsorbent dose. The optimum adsorbent dose was found to be 0.4 g/100 mL which was used for evaluation of other parameters.

Effect of initial metal concentration on removal efficiency: The influence of initial Pb^{2+} ion concentration on removal efficiency was studied with increasing amount of lead concentration solution (25-250 mg/L) against 0.4 g of iron ox-

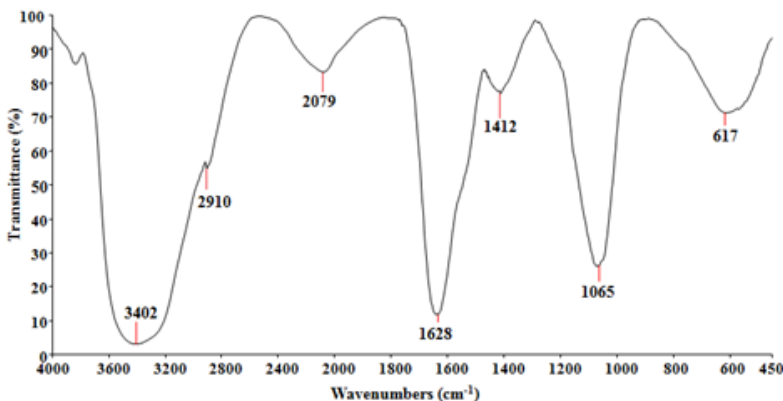
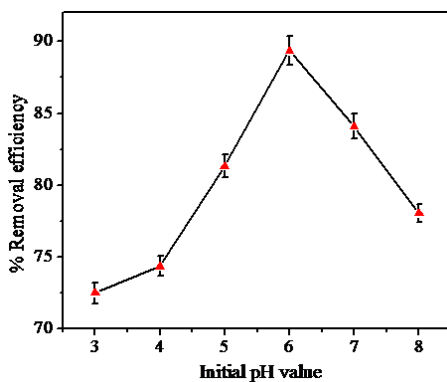
Fig. 5: FTIR spectrum of Fe_3O_4 -NPs.

Fig. 6: Effect of pH on lead removal efficiency.

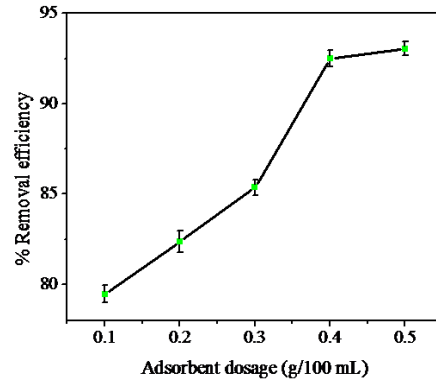


Fig. 8: Effect of adsorbent dosage on lead removal efficiency.

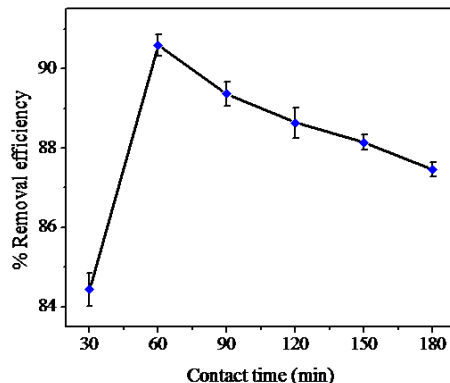


Fig. 7: Effect of incubation period on lead removal efficiency.

ide nanoparticles, at pH 6.0 for 60 min. Fig. 9 showed that there is lowering in adsorption of lead(II) ions of $93 \pm 0.13\%$ by Fe_3O_4 -NPs with increase in initial metal ion concentration of 25–250 mg/L in solution. The initial metal concentration is an important factor on the adsorption process since there are constant active binding site for a given mass of adsorbent where the fixed amount of metals can be adsorbed. Thus, increase in metal concentration in solution against same quantity of adsorbent, decreases the removal efficiency.

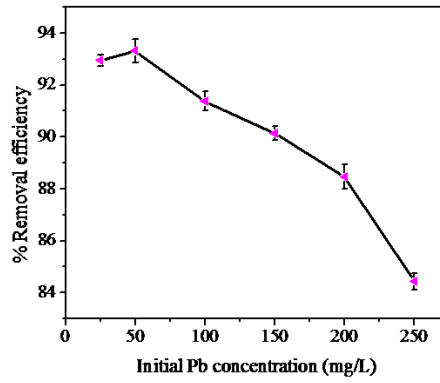


Fig. 9: Effect of initial lead concentration on heavy metal removal efficiency.

Removal of lead by Fe_3O_4 -NPs from the effluent: Adsorption of lead present in the industrial effluent was determined before and after the treatment with iron oxide nanoparticles. The results showed that excellent removal capacity of nano oxide particles. 100 % lead removal efficiency was achieved with 0.4 g of Fe_3O_4 -NPs at pH 6.0, after 60 min of incubation where initial lead concentration was found 0.1 mg/L.

Desorption studies: As heavy metals are toxic materials,

disposal of heavy metal loaded sorbent also causes environmental pollution. Thus, regeneration of adsorbent is most important step in bioremediation and biosorption process. Desorption includes regeneration of adsorbent without damaging the adsorbing capacity and recovery of metals. In this study, $99.1 \pm 0.15\%$ of adsorbed lead(II) ions desorbed within an hour, the desorption process has taken same time as sorption process. The regenerated iron oxide nanoparticles were reused and found to be efficient.

CONCLUSION

Adsorption is an efficient and economic method to remove heavy metals from contaminated water. Here, TLE were used to synthesize Fe_3O_4 -NPs and these nano oxide particles used for adsorption of Pb(II) ions from the aqueous as well as industrial effluent. Excellent heavy metal adsorption capacity together with reusability, cost-effectiveness and easy separation make Fe_3O_4 -NPs to be efficient potential adsorbing materials for heavy metal ions, and thus can be used in various industrial purification systems.

ACKNOWLEDGEMENTS

The authors convey their thanks to Department of Industrial Biotechnology, Bharath University, Chennai, for providing laboratory facilities. The authors also acknowledge SRM University, Chennai for providing support in carrying out FE-SEM, and IIT, Chennai for FTIR and XRD analysis.

REFERENCES

- Ahmed, A., Senapati, S., Islam Khan, M., Kumar, R. and Sastry, M. 2003. Extracellular biosynthesis of monodisperse gold nanoparticles by a novel extremophilic actinomycete *Thermomonospora* sp. *Langmuir*, 19: 3550-3553.
- Bai, R.S. and Abraham, E. 2003. Studies on chromium (VI) adsorption-desorption using immobilized fungal biomass. *Bioresour. Technol.*, 87: 17-26.
- Bruins, M.R., Kapil, S. and Oehme, F.W. 2000. Microbial resistance to metals in the environment. *Ecotoxicol. Environ. Saf.*, 45: 198-207.
- Bulut, Y. and Aydin, H. 2005. A kinetic and thermodynamics study of methylene blue adsorption on wheat shells. *Desalination*, 194: 259-267.
- Chang, R.P., Yu, J., Ma, X. and Anderson, D.P. 2011. Polysaccharides as stabilizers for the synthesis of magnetic nanoparticles. *Carbohydr. Polym.*, 83(2): 640-644.
- Gittins, D.I., Bethell, D., Schiffrian, D.J. and Nichols, R.J. 2000. A nanometre-scale electronic switch consisting of a metal cluster and redox-addressable groups. *Nature*, 408(6808): 67-69.
- Fayaz, M., Tiwary, C.S., Kalaichelvan, P.T. and Venkatesan, R. 2010. Blue orange light emission from biogenic synthesized silver nanoparticles using *Trichoderma viride*. *Colloids Surf. B*, 75: 175-178.
- Franger, S., Berthet, P. and Berthon J. 2004. Electrochemical synthesis of Fe_3O_4 nanoparticles in alkaline aqueous solutions containing complexing agents. *J. Solid State Electrochem.*, 8: 218-223.
- Gawande, M.B., Branco, P.S. and Varma, R.S. 2013. Nano-magnetite (Fe_3O_4) as a support for recyclable catalysts in the development of sustainable methodologies. *Chem. Soc. Rev.*, 42(8): 3371-3393.
- Hua, J. and He, Y. 2008. Qing controlled synthesis and magnetic properties of Fe_3O_4 walnut spherical particles and octahedral microcrystals. *Sci. Chin. Ser. E. Tech. Sci.*, 51: 1911-1920.
- Hua, M., Zhang, S., Pan, B., Zhang, W., Lv, L. and Zhang, Q. 2012. Heavy metal removal from water/wastewater by nanosized metal oxides: a review. *J. Hazard. Mater.*, 211-212: 317-331.
- Jose, J.V., Elias, A.M. and Saravanakumar, M.P. 2017. Carbon encapsulated zero-valent iron nanoparticle using *Abelmoschus esculentus* (lady's finger) extract as an adsorbent for Cr(VI) in aqueous solution. *Nat. Env. Poll. Tech.*, 16(1): 89-97.
- Mahdavian, A.R. and Mirrahimi, M.A.S. 2010. Efficient separation of heavy metal cations by anchoring polyacrylic acid on superparamagnetic magnetite nanoparticles through surface modification. *Chem. Eng. J.*, 159(1): 264-271.
- Paiva, D.L., Andrade, A.L., Pereira, M.C., Fabris, J.D., Domingues, R.Z. and Alvarenga, M.E. 2015. Novel protocol for the solid-state synthesis of magnetite for medical practices. *Hyperfine Interact.*, 232: 19-27.
- Prathna, T.C., Chandrasekaran, N., Raichur, A.M. and Mukherjee, A. 2011. Biomimetic synthesis of silver nanoparticles by *Citrus limon* (lemon) aqueous extract and theoretical prediction of particle size. *Colloids Surf. B*, 82: 152-169.
- Rajakumar, G. and Rahuman, A.A. 2011. Larvicidal activity of synthesized silver nanoparticles using *Eclipta prostrata* leaf extract against filariasis and malaria vectors. *Acta Tropica*, 118: 196-200.
- Repo, E., Warchol, J.K., Kurniawan, T.A. and Sillanpää, M.E.T. 2010. Adsorption of Co(II) and Ni(II) by EDTA- and/or DTPA-modified chitosan: kinetic and equilibrium modeling. *Chem. Eng. J.*, 161(1-2): 73-82.
- Selatnia, A., Boukazoula, A., Kechid, N., Bakti, M.Z., Chergui, A. and Kerchi, Y. 2004. Biosorption of lead(II) from aqueous solution by a bacterial dead *Streptomyces rimosus* biomass. *Biochem. Eng. J.*, 19: 127-135.
- Silva, R.M.P., Manso, J.P.H., Rodrigues, J.R.C. and Lagoa, R.J.L. 2008. A comparative study of alginate beads and an ion-exchange resin for the removal of heavy metals from a metal plating effluent. *J. Environ. Sci. Health A*, 43(11): 1311-1317.
- Vicky, M., Rodney, S., Ajay, S. and Hardik, M. 2010. Introduction to metallic nanoparticles. *J. Pharm. Bioall. Sci.*, 2(4): 282-289.
- Wani, I.A., Ganguly, A., Ahmed, J. and Ahmad, T. 2011. Silver nanoparticles: ultrasonic wave assisted synthesis, optical characterization and surface area studies. *Mater. Lett.*, 65: 520-522.
- Weiss, W. and Ranke, W. 2002. Surface chemistry and catalysis on well-defined epitaxial iron-oxide layers. *Prog. Surf. Sci.*, 70: 1-15.
- WHO 1984. Guideline Values for Drinking Water Quality Vol. 1, Recommendations. World Health Organization, Geneva, pp. 81.
- Zhang, Y., Das, G.K., Xu, R. and Yang Tan, T.T. 2009. Tb-doped iron oxide: bifunctional fluorescent and magnetic nanocrystals. *J. Mater. Chem.*, 19: 3696-3703.
- Zhang, Y.X., Yu, X.Y., Jin, Z., Jia, Y., Xu, W.H., Luo, T., Zhu, B.J., Liu, J.H. and Huang, X.J. 2011. Ultrahigh adsorption capacity of fried egg jellyfish-like γ -AlOOH(Boehmite) $@\text{SiO}_2/\text{Fe}_3\text{O}_4$ porous magnetic microspheres for aqueous Pb(II) removal. *J. Mater. Chem.*, 21: 16550-16557.